Science Bulletin 64 (2019) 198–204

Contents lists available at ScienceDirect

Science Bulletin

journal homepage: www.elsevier.com/locate/scib

Article

Two regimes of Atlantic multidecadal oscillation: cross-basin dependent or Atlantic-intrinsic

Pengfei Lin [a,b], Zipeng Yu [a,b], Jianhua Lü [c,*], Mengrong Ding [a,b], Aixue Hu [d], Hailong Liu [a,b,*]

[a] State Key Laboratory of Numerical Modeling for Atmospheric Sciences and Geophysical Fluid Dynamics, Institute of Atmospheric Physics, Chinese Academy of Sciences, Beijing 100029, China
[b] University of Chinese Academy of Sciences, Beijing 100049, China
[c] School of Atmospheric Sciences, Guangdong Province Key Laboratory for Climate Change and Natural Disaster Studies, Sun Yat-sen University, Guangzhou 510275, China
[d] Climate & Global Dynamics, National Center for Atmospheric Research, Boulder, CO 80301, USA

A R T I C L E I N F O

Article history:
Received 18 December 2018
Received in revised form 21 December 2018
Accepted 21 December 2018
Available online 6 January 2019

Keywords:
Atlantic multidecadal oscillation
Cross-basin interaction
Internal climate variability
AMO regimes

A B S T R A C T

The Atlantic Multidedal Oscillation (AMO) is a prominent mode of sea surface temperature variability in the Atlantic and incurs significant global influence. Most coupled models failed to reproduce the observed 50–80-year AMO, but were overwhelmed by a 10–30-year AMO. Here we show that the 50–80-year AMO and 10–30-year AMO represent two different AMO regimes. The key differences are: (1) the 50–80-year AMO involves transport of warm and saline Atlantic water into the Greenland-Iceland-Norwegian (GIN) Seas prior to reaching its maximum positive phase, while such a transport is weak for the 10–30-year AMO; (2) the zonality of atmospheric variability associated with the 50–80 year AMO favors the transport of warm and saline water into the GIN Seas; (3) the disappearance of Pacific variability weakens the zonality of atmospheric variability and the transport of warm and saline water into the GIN Seas, leading to the weakening of the 50–80-year AMO. In contrast, the 10–30-year AMO does not show dependence on the variability in Pacific and in the GIN Seas and may be an Atlantic-intrinsic mode. Our results suggest that differentiating these AMO regimes and a better understanding of the cross-basin connections are essential to reconcile the current debate on the nature of AMO and hence to its reliable prediction, which is still lacking in most of coupled models.

1. Introduction

The Atlantic Multi-decadal Oscillation (AMO) is an observed mode of sea surface temperature (SST) variability in the North Atlantic and is commonly represented by an area-weighted mean SST index of the North Atlantic (0°–65°N) [1–3]. Although the exact underlying physical mechanism for AMO is still under debate [4–6], multiple studies show that AMO is capable of generating profound impact on regional and global climate in both observations and model simulations, such as the Atlantic hurricane activity and Sahel rainfall [7–10], North American and Europe summer climate [11–13] and global warming [14–16].

Due to the lack of long-term memory in the atmosphere, it is suggested that the AMO must be associated with slow ocean processes, such as the reddening of random atmospheric variability by the large heat capacity of the oceanic mixed-layer, or be associated with the variability in Atlantic Meridional Overturning Circulation (AMOC), though there is no direct observational evidence for the AMO-AMOC linkage [17]. It is argued that the AMO is not necessarily associated with the variability of the AMOC [5]. On the other hand, the external forcings such as the variations in aerosols and greenhouse gases may also cause the AMO variability [18].

The AMO variability in instrumental observations since the late 19th century shows a salient 50–80-year period, but this particular band of low-frequency variability is often questioned due to the relatively short records. However, several long climate records indicate the existence of this multidecadal period [1,19–21]. On the other hand, most of models have difficulties in producing this 50–80-year AMO. In contrast, models show a dominant interdecadal (10–30-year) oscillation [22,23]. It has been assumed that the mechanism responsible for this 10–30-year AMO is basically the same for the 50–80-year AMO, as such the AMO is usually represented by a low-pass (longer than 10 years) filtering technique and no further distinction has been made between the different AMO frequency bands [24].

* Corresponding authors.
E-mail addresses: lvjianhua@mail.sysu.edu.cn (J. Lü), lhl@lasg.iap.ac.cn (H. Liu).

https://doi.org/10.1016/j.scib.2018.12.027
2095-9273/

However, the same spatial AMO pattern may involve fundamentally different dynamics and mechanisms, as suggested by the recent debates [5,6,25]. Some studies have suggested that the North Atlantic-Arctic connection may be responsible for the multi-decadal variability of Atlantic Meridional Overturning Circulation (AMOC), though the results were model dependent and hence suggestive [26,27].

In this paper, we show that the 50–80-year AMO and the 10–30-year AMO represent two dynamically different AMO regimes, based on our simulations, available simulations and on the reanalysis data. We further demonstrate that the 50–80-year AMO is associated with high zonality of the atmospheric variability in middle-to-high latitudes, and strongly dependent on cross-basin connections, particularly the North Atlantic-GIN-Seas connection through the cross-basin transport of warm and saline water into the GIN Seas.

2. Methods

The model used here is the Flexible Global Ocean-Atmosphere-Land System Model grid-point version 2 (FGOALS-g2) [28] with the horizontal resolution of its ocean model component LICOM2 being about 1°. The experiments include a 1,600-year control run (CTL, hereafter) with all forcings fixed at pre-industrial (1850) level, and two partially coupled sensitivity experiments, in which the ocean temperature of the full depth in the tropical Pacific (20°S–20°N, denoted as TPdepth experiment) or North Pacific (20°N–65°N, denoted as NPdepth experiment) is restored back to the climatological monthly mean state of the CTL run so as to mute the variability in the tropical Pacific (ENSO) or in the North Pacific (PDO) and their influences on AMO. The outputs from HadGEM2-ES, direct observational data and atmospheric and oceanic reanalysis data are also used to confirm the results (see Methods and Table S1 online for more details). Note FGOALS-g2 is one of the four "most accurate" CMIP5 models in terms of both the location and the variability of deep water formation in North Atlantic [29]. Further Details about Method see Supplementary Data Methods (online).

3. Results

The simulated AMO pattern in all of the three experiments is a basin wide warming/cooling in the North Atlantic (Fig. 1a–c) derived from the regression of SST onto the AMO index [8], a pattern close to the observations [8]. The simulated AMO in CTL run has a statistically significant (at around 95% confidence level) period of 50–80 years (Fig. 1d), similar to the observed AMO during 20th century (Fig. S1 online), but the 50–80-year AMO disappears largely when either the PDO or the ENSO is muted, while the 10–30-year AMO remains in the TPdepth and NPdepth experiments (Fig. 1e and f).

The different responses of the 50–80-year and 10–30-year AMOs to the muted Pacific variability imply different AMO regimes associated with different underlying dynamics. To compare the associated atmospheric variability in the three experiments, the corresponding atmospheric fields are regressed onto the AMO index of 50–80-year period (Fig. 2a–f) and 10–30-year period (Fig. 2g–l). The atmospheric variability associated with the 50–80-year AMO in CTL (Fig. 2a and d) shows a zonally coherent structure over the globe. Associated with a positive AMO at 50–80-year period the westerlies are enhanced north of 60°N, but weakened between 40°N and 60°N which are dynamically consistent with an enhanced polar vortex. Meanwhile there is a belt of enhanced precipitation along the Intertropical Convergence Zone (ITCZ) extending from the tropical Indian Ocean and western Pacific northwestward to tropical Atlantic. In particular the zonal structure of the ITCZ anomaly for the 50–80-year AMO in our model is similar to that obtained from reanalysis data (Fig. S2 online). Such a zonally coherent structure in the atmospheric variability associated with the 50–80-year AMO, which is statistically insignificant in both of the sensitivity experiments, disappears in the TPdepth experiment (Fig. 2b and e) and NPdepth experiment (Fig. 2c and f), such as the regression coefficients between low-level zonal wind, 500-hPa geopotential height and 50–80-year AMO reduced by over 40% in these experiments relative to that in CTL. Hence the mute of variability in tropical or northern Pacific sea temperature weakens or even destroys the zonal coherence of extratropical variability. The possible role of zonally coherent atmospheric variability in the 50–80 year AMO will be further analyzed in detail near the end of the paper.

The atmospheric variability associated with the 10–30-year AMO in CTL (Fig. 2g and j) is a zonally asymmetric pattern with blockings prevailing over high latitude North Atlantic, cyclonic anomaly over subtropical North Atlantic, and enhanced precipitation over tropical Atlantic. As shown in Fig. 2g–l, the atmospheric variability related to 10–30-year AMO in all three experiments are similar to each other, implying that the 10–30-year AMO is basically independent from the variability over Pacific sector. Based on the strongest signal occurring over the North Atlantic and the independence from Pacific variability, the 10–30-year AMO might be a mode of variability intrinsic to Atlantic only. This may explain why the 10–30-year AMO largely remains unchanged in the experiments with muted Pacific variability.

To understand the possible mechanisms behind these two AMO regimes, we start by rechecking the spatial pattern of the AMO. Although the same spatial pattern has been depicted in the 50–80-year and 10–30-year AMOs by band-pass-filtering the time-series of original AMO, new spatial patterns may be obtained by regressing the gridded SST upon the filtered AMO time series separately for the two frequency bands. While both spatial patterns are similar to the original one, some important differences emerge. The SST pattern of the 50–80-year AMO (Fig. 3a) has stronger signal over the GIN Seas, but a weaker signal over the tropics than that of 10–30-year AMO (Fig. 3b). This structural difference in the two AMO regimes exists in both observations (Fig. 3e and f for ERSST-v3b) and other coupled simulations, which can also produce 50–80-year AMO (Fig. 3c and d for HadGEM2-ES). This robust difference of the AMO regimes in both observations and model simulations suggests that while the 10–30-year AMO may be linked directly to the dynamics over the tropical Atlantic, the 50–80-year AMO is heavily related to the cross-basin interaction between the North Atlantic and the GIN Seas. The salinity pattern associated with the 50–80-year AMO also has stronger signal in the GIN Seas and even the Arctic than that with the 10–30-year AMO (Fig. S3 online).

With the basic structure of ocean circulation in the north Atlantic in mind, it is very natural to conjecture that the North Atlantic-GIN Seas connection in the 50–80-year AMO should be related to variability in northward transport of warm and saline water into the GIN Seas and their southward returning to the North Atlantic, while no such coherent transport into the GIN Seas is involved in the 10–30-year AMO. Indeed this is exactly the case. The first EOF of 50–80-year filtered annual-mean barotropic streamfunction (BSF, Fig. 4a) in CTL shows a coherent cyclonic variability in the subpolar gyre region extending to the GIN Seas with opposite variability in the ocean near the southern tip of Greenland. When the 50–80-year AMO is regressed onto the BSF field with the latter leading the former by half-period (30 years, Fig. 4b), the resulting regression pattern is very close to the first EOF of the 50–80-year band-pass-filtered BSF. This illustrates that a cumulative transport of warmer and saltier upper ocean water into the GIN Seas in ear-

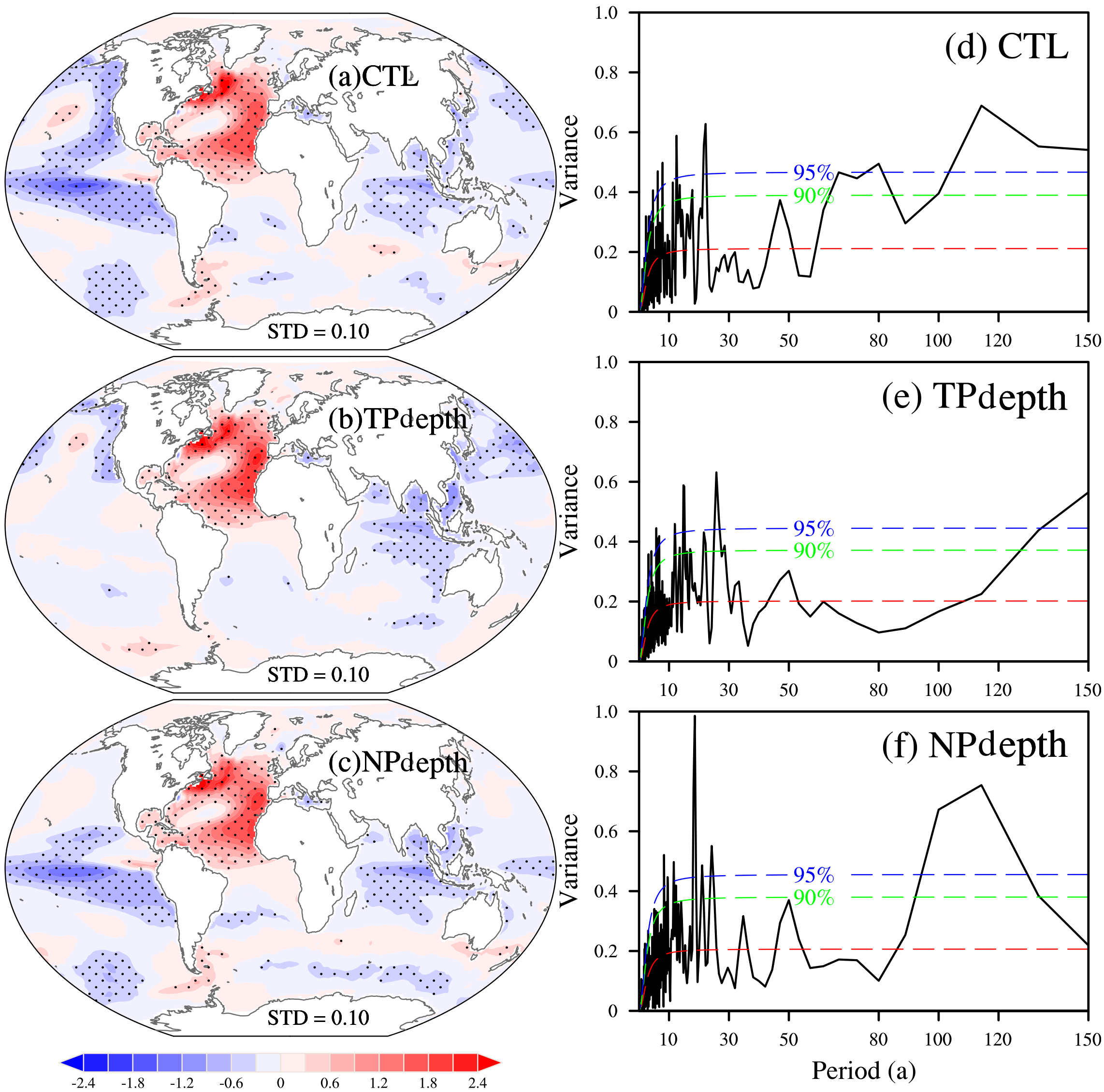

Fig. 1. AMO SST patterns (left panel) and corresponding power spectra (right panel) of AMO indexes in the CTL (a, d), TPdepth (b, e) and NPdepth (c, f) experiments. The monthly AMO index is defined as the detrended North Atlantic (0°–60°N, 80°W–0°) monthly SST anomalies minus global (60°S–60°N) mean monthly SST [8]. The pattern is obtained by regressing monthly SST anomalies onto the AMO index and then smoothing it with a 9-point spatial filter. The dots indicate the magnitude of the regression is above 0.3. The red and blue curves are red-noise test and the 5% significance test, respectively.

lier decades will result in a subsequent positive phase of the 50–80-year AMO. By contrast, both the first EOF of the 10–30-year filtered BSF (Fig. 4c) and the regression pattern of BSF which is regressed upon the 10–30-year AMO with the former leading the latter by around half-period (10 years, Fig. 4d) exhibit a meridional tripole structure extending from the GIN Seas to the subpolar gyre region and to the subtropical gyre region, which is not favorable for the transport of warm and saline water into the GIN Seas and the Arctic. Hence the North Atlantic-GIN Seas connection or the transport of warm and saline water into the GIN region forms a major feature of the 50–80-year AMO different from the 10–30-year AMO.

Now we may explain the disappearance of the 50–80-year AMO in TPdepth and NPdepth experiments. Note the zonal symmetry of the atmospheric variability associated with the 50–80-year AMO not only appears in the simultaneous regression (Fig. 2a), but also prevails in lead-lag regressions (Fig. S4 online). About half-period (30 years) prior to the maximum positive phase of AMO (AMO_{max+}), a negative NAO-like pattern prevails in the northern high-latitudes accompanied by enhanced westerly near 30°N and easterly anomalies between 40° and 60°N (Fig. S4a online), and also by the positive ocean heat content (OHC) and salinity anomalies in between the surface and 300 m depth (Fig. S4b and c online) in the Labrador Sea and the GIN Seas. This atmospheric pattern, i.e., the northern cyclonic and southern anticyclonic anomalies, is dynamically consistent with the regressed oceanic BSF in Fig. 4b, indicating an enhanced subpolar gyre and enhanced transport of warm and saline water to the GIN Seas (Fig. S4b and c online), consistent with recent observational and modeling study [30]. The similar pattern lasts more than 15 years as shown in Fig. S4d–f (online), until about 8 years prior to the AMO_{max+}, when the pattern reverses to opposite sign. These features, and the quantitative zonality measurement (Table 1) shows that the zonality of atmospheric variability associated with the 50–80-year AMO is much larger than that of 10–30-year AMO, suggesting that the 50–80-year AMO is a cross-basin dependent mode of multidecadal

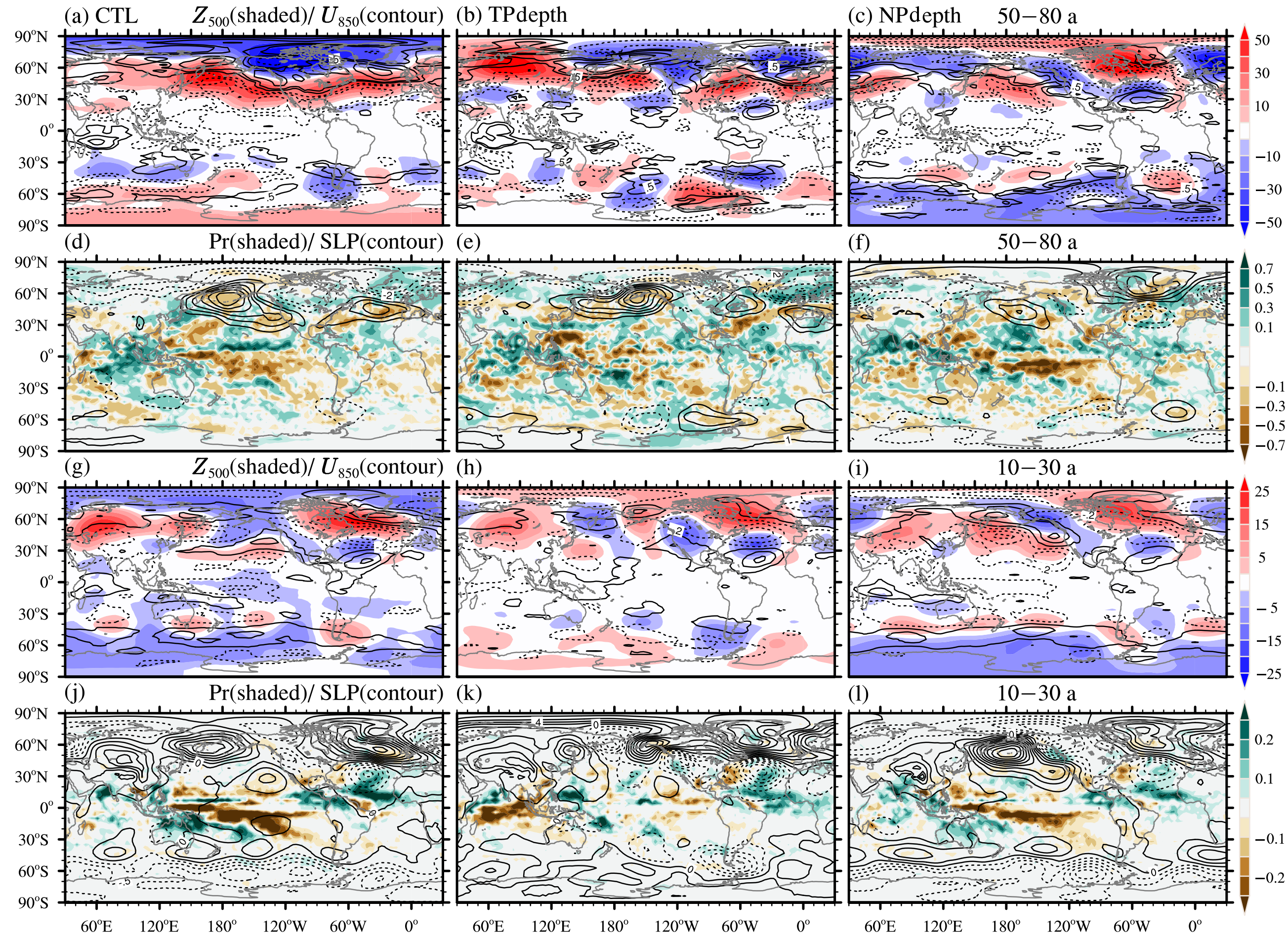

Fig. 2. The simultaneous regressions of atmospheric fields regressed onto the 50–80-year AMO (a–f) and onto the 10–30-year AMO (g–l). The left column for CTL, the middle column for TPdepth experiment, and the right column for NPdepth experiment. The atmospheric fields include winter (December-January-February, DJF) Z_{500} (shading, gpm/0.1 K) and U_{850} (line contours, m/(s 0.1 K)) in the first and third rows, annual-mean precipitation (shading, mm/(d 0.1 K)) and DJF sea level pressure (SLP, line contours, hPa/0.1 K) in the second and fourth rows. The intervals of line contours for U_{850} (SLP) are 2 m/(s 0.1 K) (hPa/0.1 K) for the 50–80-year AMO and 0.4 m/(s 0.1 K) (hPa/0.1 K) for the 10–30-year AMO. The dashed contours represent negative values.

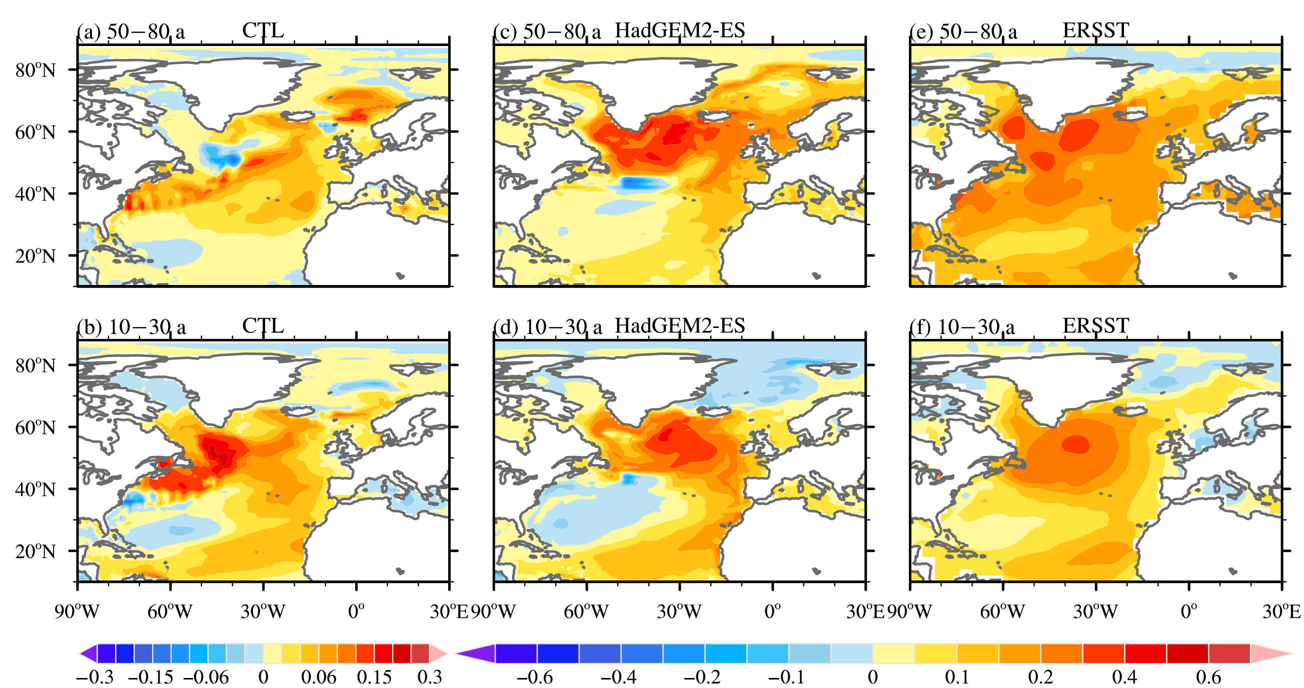

Fig. 3. The 50–80-year AMO (upper panel) and 10–30-year AMO SST (lower panel) patterns. (a), (b) CTL; (c), (d) HadGEM2-ES; (e), (f) ERSST-v3b. The patterns are obtained by regressing monthly SST anomalies onto the 50–80-year or 10–30-year band-pass-filed AMO index and then smoothing it with a 9-point spatial filter. Unit: K.

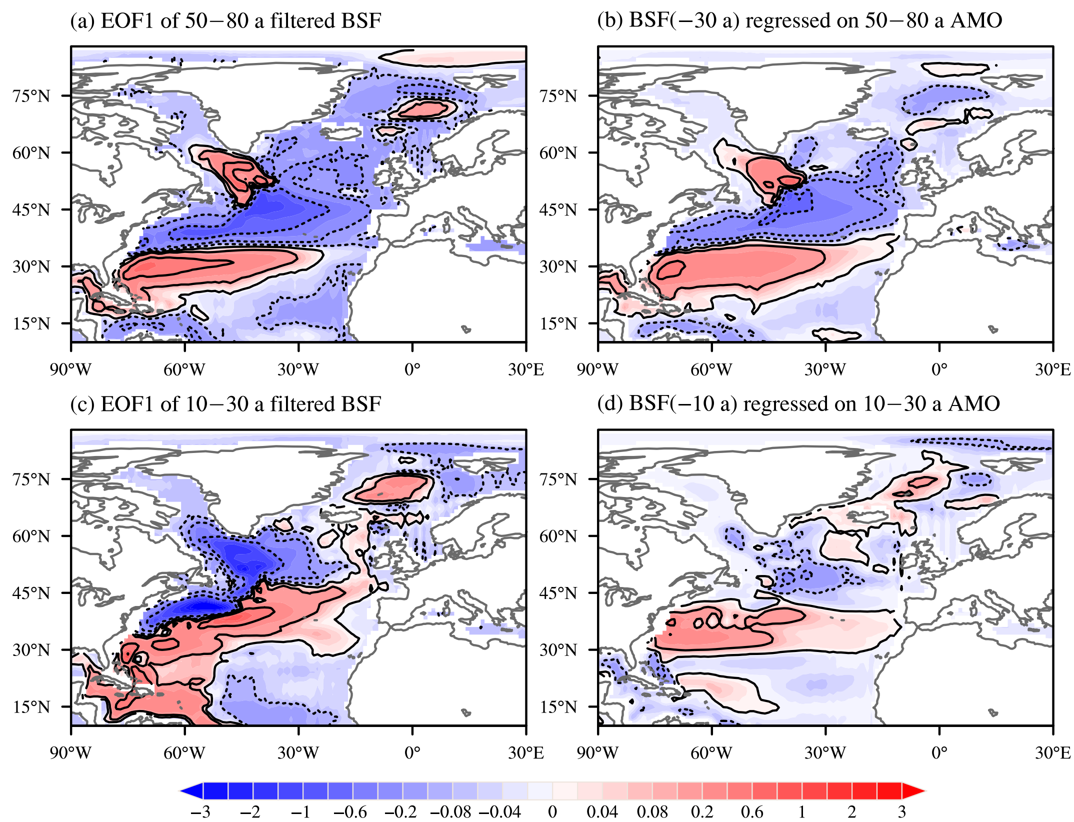

Fig. 4. The first EOFs of barotropic streamfunction (BSF) at different frequency bands (50–80-year for (a), 10–30-year for (c)) and the leading BSFs regressed onto the AMO indexes at different leading time (30 years for (b) and 10 years for (d)). Unit for (a) and (c): Sv per standard deviation of the first principal component (PC1); unit for (b) and (d): Sv per standard deviation of the AMO.

Table 1
The zonality of the lead-lag regressions of U_{850} (between 45° and 65°N) and Z_{500} (between 30° and 60°N) regressed onto the 50–80-year AMO and 10–30-year AMO.

	50–80-year AMO		10–30-year AMO	
	U_{850}	Z_{500}	U_{850}	Z_{500}
CTL	1.913	1.342	0.656	0.824
TPdepth	0.943	0.829	0.700	0.506
NPdepth	0.757	0.374	1.151	0.586

variability. Indeed the zonality of atmospheric variability associated with the 50–80-year AMO in both the HadGEM2-ES (1.269 for U_{850}) simulation and reanalysis (1.357 for Z_{500}) is also larger than their counterparts (0.42 for U_{850} in HadGEM2-ES and 0.08 for Z_{500} in reanalysis) for the 10–30-year AMO. We may infer that, because the muting of Pacific variability destroys the zonality or global coherence of atmospheric variability (Table 1), and weakens the transport of warm and saline water into the GIN Seas, the 50–80-year AMO largely disappears in the TPdepth and NPdepth experiments.

In contrast, not only the lead-lag regressions of the atmospheric and oceanic variability onto the 10–30-year AMO do not indicate zonally coherent structures (Table 1 and Fig. S5 online), but also the positive SST and salinity anomalies do not spread into the GIN Seas and the Arctic (Fig. S5 online). This further confirms, together with the simultaneous regressions in Fig. 2g–l, that the 10–30-year AMO is an Atlantic-intrinsic mode, and hence basically independent from the variability in other ocean basins. Therefore the 10–30-year AMO remains in the partially coupled sensitivity experiments with Pacific variability being muted (Fig. 1e and f).

4. Conclusions and discussion

By comparing the AMO variability between fully coupled CTL and partially coupled sensitivity runs with muted ocean temperature variability in the tropical or North Pacific, we show a disappearance of the 50–80-year AMO, indicating this 50–80-year AMO is a cross-basin dependent mode. Evidence from available model simulations and reanalysis confirm that enhanced and an extended subpolar gyre transports warm and saline water northward into the GIN Seas starting from about half-period prior to the 50–80-year AMO_{max+}, accompanied by a zonally coherent atmospheric variability, and then the positive SST and salinity anomalies spread across the entire North Atlantic. This North Atlantic-GIN Seas connection is a robust feature of 50–80-year AMO, confirmed by both observations and other available simulations. In contrast, the 10–30-year AMO neither shows dependence on the variability in Pacific nor involves a strong transport of warm and saline water into the GIN Seas and the Arctic, and hence it may be an Atlantic-intrinsic mode associated with Atlantic-based variability only.

Our results suggest that cautions should be taken in using the underlying mechanisms obtained by most of the models, in which the 10–30-year AMO dominates, to explain the 50–80-year AMO in observations. Distinguishing the AMO regimes may help to clarify oft-contradictory reports on the relations among NAO, AMOC, and AMO [31–33]. Our results also suggest that the key factor responsible for most model's weakness in simulating AMO may be the atmospheric and oceanic processes linking the North Atlantic, GIN Seas, and even the Arctic together. The intriguing complexity in the internal dynamics of atmospheric and oceanic variabilities and their interactions over the GIN Seas and North Atlantic or even the globe at large, while providing the AMO rich flavors, requires not only coordinated observations and modeling studies [33], but also better framework of theoretical understanding.

Conflict of interest

The authors declare that they have no conflict of interest.

Acknowledgments

This work was supported by the National Key R&D Program for Developing Basic Sciences (2016YFC1401401, 2016YFC1401601, Y83A01c801), Sun Yat-Sen University's "Hundred Talents" Program, the National Natural Science Foundation of China (41576026 and 41576025), the Regional and Global Model Analysis (RGMA) under the Earth and Environmental System Modeling Program of the U.S. Department of Energy's Office of Biological & Environmental Research (BER) Cooperative Agreement (DE-FC02-97ER62402). National Center for Atmospheric Research is sponsored by National Science Foundation of the United States of America. We acknowledge CMIP5 program and the HadGEM group in U. K. make the HadGEM2-ES simulation available.

Author contributions

Jianhua Lü originated and developed the concept. Jianhua Lü and Pengfei Lin designed the experiments, led the analysis, and wrote the manuscript. Pengfei Lin performed the experiments. Zipeng Yu and Mengrong Ding performed the model and statistical analysis. Hailong Liu co-designed the experiments and organized the resources for the research in State Key Laboratory of Numerical Modeling for Atmospheric Sciences and Geophysical Fluid Dynamics. All authors contributed to the shaping and production of the manuscript.

Appendix A. Supplementary data

Supplementary data to this article can be found online at https://doi.org/10.1016/j.scib.2018.12.027.

References

[1] Schlesinger ME, Ramankutty N. An oscillation in the global climate system of period 65–70 years. Nature 2000;367:723–6.
[2] Kerr RA. A North Atlantic climate pacemaker for the centuries. Science 2000;288:1984–5.
[3] Knight JRR, Allan J, Folland CK, et al. A signature of persistent natural thermohaline circulation cycles in observed climate. Geophys Res Lett 2005;32:L20708.
[4] Chen H, Schneider EK, Wu Z. Mechanisms of internally generated decadal-to-multidecadal variability of SST in the Atlantic Ocean in a coupled GCM. Clim Dyn 2016;46:1517–46.
[5] Clement AC, Bellomo K, Murphy LN, et al. The Atlantic Multidecadal Oscillation without a role for ocean circulation. Science 2015;350:320–4.
[6] Zhang R, Sutton R, Danabasoglu G, et al. Comment on "the Atlantic Multidecadal Oscillation without a role for ocean circulation". Science 2016;352:1527.
[7] Goldenberg SB, Landsea CW, Mestas-Nuñez AM, et al. The recent increase in Atlantic hurricane activity: causes and implications. Science 2001;293:474–9.
[8] Trenberth KE, Shea DJ. Atlantic hurricanes and natural variability in 2005. Geophys Res Lett 2006;33:L12704.
[9] Zhang R, Delworth TL. Impact of Atlantic Multidecadal Oscillations on India/Sahel rainfall and Atlantic hurricanes. Geophys Res Lett 2006;33:L17712.
[10] Ting M, Kushnir Y, Seager R, et al. Robust features of Atlantic multi-decadal variability and its climate impacts. Geophys Res Lett 2011;38:L17705.
[11] Enfield DB, Mestas-Nuñez AM, Trimble PJ. The Atlantic Multidecadal Oscillation and its relation to rainfall and river flows in the continental U.S. Geophys Res Lett 2001;28:2077–80.
[12] Sutton RT, Hodson DLR. Atlantic Ocean forcing of North American and European summer climate. Science 2005;309:115–8.
[13] Knight JR, Folland CK, Scaife AA. Climate impacts of the Atlantic Multidecadal Oscillation. Geophys Res Lett 2006;33:L17706.
[14] DelSole T, Tippett MK, Shukla J. A significant component of unforced multidecadal variability in the recent acceleration of global warming. J Clim 2011;24:909–26.
[15] Chikamoto Y, Kimoto M, Watanabe M, et al. Relationship between the Pacific and Atlantic stepwise climate change during the 1990s. Geophys Res Lett 2012;39:L21710.
[16] Chen X, Tung KK. Varying planetary heat sink led to global-warming slowdown and acceleration. Science 2014;345:897–903.
[17] Lozier MS. Deconstructing the conveyor belt. Science 2010;328:1507–11.
[18] Booth BBB, Dunstone NJ, Halloran PR, et al. Aerosols implicated as a prime driver of twentieth-century North Atlantic climate variability. Nature 2012;484:228–32.
[19] Gray ST, Graumlich LJ, Betancourt JL, et al. A tree-ring based reconstruction of the Atlantic Multidecadal Oscillation since 1567 A.D. Geophys Res Lett 2004;31:L12205.
[20] Tung KK, Zhou J. Using data to attribute episodes of warming and cooling in instrumental records. Proc Natl Acad Sci USA 2013;110:2058–63.
[21] Mjell TL, Ninnemann US, Kleiven HF, et al. Multidecadal changes in Iceland Scotland Overflow Water vigor over the last 600 years and its relationship to climate. Geophys Res Lett 2016;43:2111–7.
[22] Peings Y, Simpkins G, Magnusdottir G. Multidecadal fluctuations of the North Atlantic Ocean and feedback on the winter climate in CMIP5 control simulations. J Geophys Res Atmos 2016;121:2571–92.
[23] Ruiz-Barradas A, Nigam S, Kavvada A. The Atlantic Multidecadal Oscillation in twentieth century climate simulations: uneven progress from CMIP3 to CMIP5. Clim Dyn 2013;41:3301–15.
[24] Delworth TL, Zeng F, Zhang L, et al. The central role of ocean dynamics in connecting the North Atlantic Oscillation to the extratropical component of the Atlantic Multidecadal Oscillation. J Clim 2017;30:3789–805.
[25] Cane M, Clement AC, Murphy LN, et al. Low-pass filtering, heat flux, and Atlantic multidecadal variability. J Clim 2017;30:7529–53.
[26] Jungclaus JH, Haak H, Latif M, et al. Arctic-North Atlantic interactions and multidecadal variability of the meridional overturning circulation. J Clim 2005;18:4013–31.
[27] Frankcombe LM, Heydt von der A, Dijkstra HA. North Atlantic multidecadal variability: an investigation of dominant time scales and processes. J Clim 2010;23:3626–38.
[28] Li LJ, Lin PF, Yu YQ, et al. The flexible global ocean-atmosphere-land system model, grid-point version 2: FGOALS-g2. Adv Atmos Sci 2013;30:543–60.
[29] Heuze C. North Atlantic deep water formation and AMOC in CMIP5 models. Ocean Sci 2017;13:609–22.
[30] McCarthy GD, Haigh ID, Hirschi JJ, et al. Ocean impact on decadal Atlantic climate variability revealed by sea-level observations. Nature 2015;521:508–10.
[31] Li J, Sun C, Jin FF. NAO implicated as a predictor of Northern Hemisphere mean temperature multidecadal variability. Geophys Res Lett 2013;40:5497–502.
[32] Buckley MW, Marshall J. Observations, inferences, and mechanisms of the Atlantic meridional overturning circulation: a review. Rev Geophys 2016;54:5–63.
[33] Sutton RT, McCarthy GD, Robson J, et al. Atlantic multidecadal variability and the U.K. ACSIS Program. Bull Amer Meteorol Soc 2018;99:415–25.

Pengfei Lin is an associate research scientist in the Institute of Atmospheric Physics (IAP), Chinese Academy of Sciences (CAS). He received his M.S. from Institute of Oceanology, CAS and Ph.D. from IAP, CAS. He had visited Woods Hole Oceanographic Institute, Maine University and National Center for Atmospheric Research. He focuses on the roles of ocean in climate variability and climate change and also ocean model development.

Jianhua Lü obtained his Ph.D. degree in meteorology from Institute of Atmospheric Physics, Chinese Academy of Sciences in 1999. He has been a professor in School of Atmospheric Sciences, Sun Yat-sen University since 2016, after a decade-long studying abroad in the field of climate science. His research interests are mainly in the theory and modeling of atmospheric, oceanic, and climate dynamics across various spatiotemporal scales.

Hailong Liu obtained his Ph.D. degree in meteorology from the University of Chinese Academy of Sciences (UCAS) in 2002. In the same year, he began his research career in Institute of Atmospheric Physics (IAP), Chinese Academy of Sciences and now holds the position of Research Fellow in IAP and the Professor in UCAS. His researches are focused on the development and application of the ocean general circulation model and the study of the ocean's role in the climate system.